*J. Fluid Mech.* (1974), *vol.* 66, *part* 2, *pp.* 309–337
*Printed in Great Britain*



# On transition mechanisms in vertical natural convection flow

By YOGESH JALURIA† AND BENJAMIN GEBHART
Sibley School of Mechanical and Aerospace Engineering, Cornell University, Ithaca, New York 14850

(Received 2 July 1973 and in revised form 28 March 1974)

An experimental investigation has been made of the processes occurring during the natural transition from laminar to turbulent flow of natural convection flow of water adjacent to a flat vertical surface where the surface heat flux is uniform. Measurements of both the velocity and temperature fields were made over wide ranges of the heat flux and at various downstream locations. Of principal interest were the definitions of the boundaries of the transition regime and their determination at several values of the surface heat flux. The interaction of the velocity and temperature fields during transition was measured. Our results show that transition events are not correlated in terms of the Grashof number $G^*$. The form $G^*/x^n$, where $n$ is of order $\frac{1}{2}$, was found to give satisfactory correlations. Measurements of the frequency and growth rate of disturbances indicate the primacy of the velocity field during transition and show that the growth of turbulence in the temperature field lags behind that in the velocity field. The study of the turbulence growth, in terms of intermittency factors in both the velocity and temperature fields, resulted in unambiguous criteria for the boundaries of the transition regime. Our results suggest a kinetic energy flux parameter $E$ and a single value closely correlates both our measurements of the onset of transition as well as those from all past studies known to us, for both different fluids and heating conditions.

## 1. Introduction

Recent years have seen a growing interest in natural convection boundary-layer flows. However, most studies have been concerned with laminar flow or with only the earlier stages in the long process of the conversion of laminar flow to turbulence. Although there has been some investigation of the turbulent regime, the basic processes underlying the final stages of breakdown are still largely unknown. As turbulent flows are often of greater practical significance in nature and in technology, it is important to understand when and how laminar flows finally become turbulent.

The early stages of disturbance amplification were initially considered from the standpoint of linear stability. The question concerns the conditions under which a balance of buoyancy, pressure and viscous forces contributes energy to a disturbance and causes its growth as it is convected downstream. It is believed

† Present address; Engineering Research Center, Western Electric Co., Inc., P.O. Box 900, Princeton, New Jersey 08540, U.S.A.

that later breakdown of laminar flow follows from such highly amplified disturbances. The extensive analytical and experimental investigation of recent years concerning laminar instability has been summarized by Gebhart (1973).

The analytical predictions of both the initial instability and the early growth rate of disturbances have received excellent corroboration from experimental studies. A very important result of these studies, for flows adjacent to vertical surfaces, is that only disturbances in a very narrow band of frequencies are rapidly amplified downstream.

As a disturbance amplifies downstream, three-dimensional and nonlinear effects become important. The analysis of Audunson & Gebhart (1975) includes both effects for a Prandtl number $Pr$ of 0·7. The experimental investigation of Jaluria & Gebhart (1973) in water, $Pr = 6{\cdot}7$, and with controlled disturbances substantiated many of the predictions of that analysis. Both analysis and experiment have shown that the nonlinear interactions among three-dimensional disturbances lead to the establishment of a secondary mean flow consisting of a double longitudinal vortex system. The outer vortex was found to stretch out across the boundary region and into the ambient medium. An alternate spanwise steepening and flattening of the longitudinal mean velocity profile results. It was inferred that this distortion would lead to higher local rates of energy transfer to disturbances, causing a more rapid growth. Thus, we now believe that nonlinear interactions give rise to a secondary mean motion, which in turn may lead to breakdown and the onset of transition.

However, few experimental studies have been made of the mechanism of actual transition in natural convection. Some experimental data concerning turbulent flow exist, but most of them are in the form of overall heat-transfer rates and mean temperature profiles. Griffiths & Davis (1922) made the first measurements of local heat transfer, as well as of mean velocity and temperature, in air adjacent to an isothermal vertical surface. Recently Cheesewright (1968) and Warner (1966) made a more detailed study of the same case, confirming and extending the earlier results. The emphasis was again on the temperature field, in particular on heat-transfer rates and mean temperature profiles. However, these studies dealt primarily with turbulent flow; few measurements were made in the transition regime. Cheesewright also made some velocity measurements, but no data were taken in the transition region. The appearance of significant temperature fluctuations was taken as the beginning of transition. The end of transition was simply taken as the downstream location where major changes in the form of the mean temperature profiles ended.

Vliet & Liu (1969) and Lock & de B. Trotter (1968) made more detailed studies of turbulent natural convection flow adjacent to a uniform-heat-flux vertical surface in water. They also made some temperature measurements during transition. Vliet & Liu defined the beginning of transition to be the downstream location where the surface temperature begins to decrease from a maximum value. Some velocity data are given for the turbulent regime. Lock and de B. Trotter measured temperature distributions and inferred the scale and intensity of the turbulence. They also obtained some intermittency data from their temperature measurements.

A significant point that emerges from past studies is the wide range of Grashof numbers over which both the beginning and end of transition have been estimated to occur. For a uniform-heat-flux surface, the Grashof number $G^*$ is here defined as $G^* = 5(g\beta_T q'' x^4/5k\nu^2)^{\frac{1}{5}}$, where $x$ is the distance along the vertical surface from the leading edge, $q''$ the uniform surface heat flux, $k$ the thermal conductivity, $\nu$ the kinematic viscosity, $\beta_T$ the coefficient of thermal expansion and $g$ the acceleration due to gravity. The relation between $G^*$ and the conventional Grashof number $Gr_x$ is given in the appendix.

Linear stability theory predicts that the downstream growth rate of a two-dimensional disturbance depends, for a given Prandtl number, only on $G^*$. It is, therefore, important to determine whether a systematic trend does exist in the $G^*$ values at the beginning and end of transition and if these values vary with either the heat flux $q''$ or the value of $x$ at which measurements are taken.

A preliminary investigation of this question is reported by Godaux & Gebhart (1974) in a study of the temperature field during transition. Defining the beginning of thermal transition as the point where the mean temperature profile begins to change its form from the laminar one, they found that the local $G^*$ at the beginning of transition varied about as $x^{\frac{3}{5}}$. That is, transition occurred near a constant value of $G^*/x^{\frac{3}{5}} \propto (q''x)^{\frac{1}{5}}$. The end of transition was not as well defined in their measurements and a range of $G^*$ was suggested.

It is very significant that this trend was found even though the beginning of transition is not sharply defined nor easily measured in terms of a departure from laminar mean flow distributions. Nor is this the usual definition. The more common practice is to take the first appearance of turbulent bursts as the onset of transition as is widely done in forced flows; see, for example, Tani (1969). In addition, since no detailed velocity measurements were made by Godaux & Gebhart, no conclusions could be drawn regarding the nature of either the velocity field or of the details of its interaction with the temperature field.

Clearly, an extensive investigation was needed to determine detailed transition mechanisms and to find any relation which may exist between what is now known of instability and disturbance growth, on the one hand, and eventual transition, on the other. Such a study would determine the gross features of the boundary-region flow as well as the nature and behaviour of the disturbances as the flow undergoes transition. A principal aspect of this problem is the way the velocity and temperature fields interact and influence each other. This requires an investigation of the frequency and growth of disturbances as well as of the onset and development of turbulence in the two overlapping boundary regions. Thus far, this question has not been considered, and we shall see that it is of great significance in water, owing to the large disparity in the thicknesses of the two laminar boundary regions. Another important question is how the $G^*$ values defining the limits of transition vary with $q''$ or $x$. Our measurements cover the whole transition regime in a flow subject only to naturally occurring disturbances.

Past and new information have led us to formulate the sequence of events shown in figure 1. Turbulence, or bursts, were found to occur first in the thicker velocity region, then later in the temperature field. Further downstream, the mean velocity profile was found to change its form from the laminar one and to

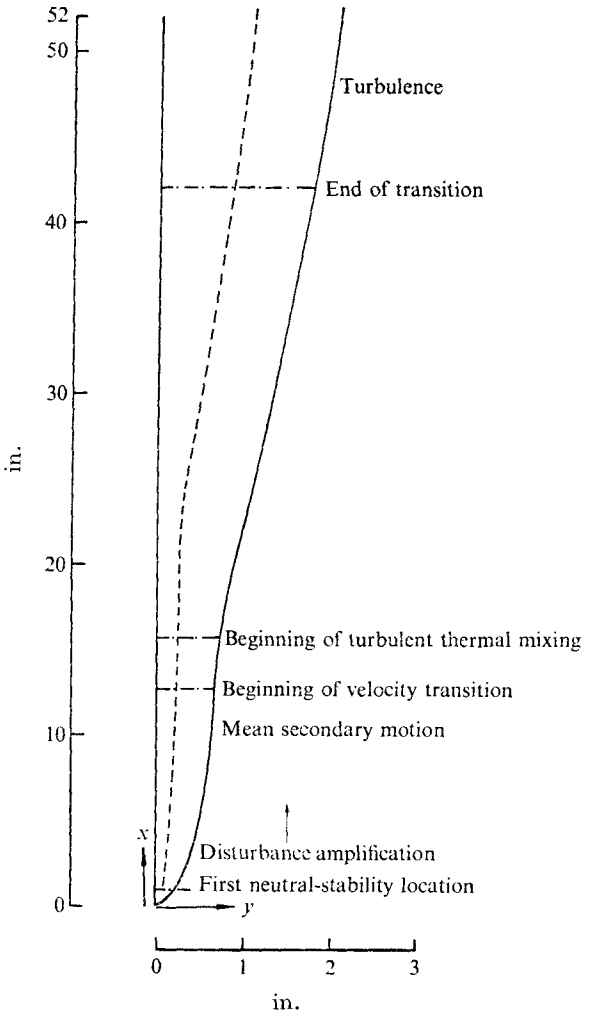


FIGURE 1. Growth of boundary-layer thickness and sequence of events during transition in water ($Pr$ = 6·7) at $q''$ = 300 B.Th.U./h ft$^2$.

reach out further into the ambient medium. This was later accompanied by a major distortion of the mean temperature profile, the beginning of what Godaux & Gebhart (1974) called 'thermal' transition.

The growth of turbulence is expressed in terms of the local intermittency factor $\Gamma(x, y)$, the fraction of time that the flow is turbulent at a downstream location $x$ and boundary-region location $y$. It was determined separately for the velocity ($\Gamma_V$) and temperature ($\Gamma_T$) fields. We shall see that the end of transition is defined as the downstream location $x$ beyond which both intermittency factors, at the measured edge of the respective boundary regions, no longer change appreciably in magnitude. This implies an unchanging distribution of $\Gamma_V$, or of $\Gamma_T$, when plotted against the normal distance $y$ from the surface, when $y$ is normalized by the corresponding measured mean boundary-layer thickness $\delta_{VM}$ or $\delta_{TM}$. Two limits separately indicate an end of transition

in velocity and in temperature. Our measurements have shown that these two different measures of the end of transition coincide.

We have also measured the predominant frequencies of the velocity and temperature disturbances. The mean temperature and velocity profiles, and the growth of the corresponding boundary-layer thicknesses, were measured. The distribution of disturbance amplitude across the boundary region was also obtained. We also measured disturbance intensities during transition. The measurements were made over wide ranges of the downstream location $x$ and of the uniform surface heat flux $q''$.

The present results indicate that flow and temperature characteristics in the transition regime are not properly correlated in terms of the parameter $G^*$ and that the downstream location $x$, or the surface flux $q''$, must be considered in conjunction with $G^*$ for a better correlation. The results indicate that the parameter $G^*/x^n$, where $n$ lies between 0·4 and 0·54, is an accurate correlating factor. Its physical significance is discussed.

## 2. The experiment

The experiment was carried out in flow adjacent to a uniform-flux flat vertical surface. The flat surface which generated the flow was a 52 in. high and 19·8 in. wide Inconel 600 foil assembly consisting of two foils 0·0005 in. thick separated by layers of teflon. The assembly was bonded at high pressure and temperature to fuse the teflon. This gave a very flat surface, which was then stretched vertically between two knife edges. This arrangement gave rise to a well-defined boundary layer on both sides. The foil assembly was heated electrically by means of a d.c. motor generator when the current required was 30 A or more and by an electronic d.c. power supply for smaller currents. Both the power supplies were very stable and our measurements of velocity and temperature indicated no dependence on the power supply used. The voltage across the foil was measured by a digital voltmeter and the current through it by means of a shunt resistance in series. As the flux is obtained from electrical dissipation, the condition of uniform surface flux is achieved for a foil of uniform thickness.

The investigation was carried out in a $6 \times 2\frac{1}{2} \times 6$ ft high insulated tank made of stainless steel, with glass windows. The leading edge of the foil was 5·7 in. from the bottom of the tank and the trailing edge 15 in. from the water surface. A water purification and deaeration system enabled us to increase the resistivity level of the water in the tank to around 1 MΩ cm. The system is described in detail by Hollasch (1970). Water of such a high purity is needed to avoid 'drift' in the calibration of bare hot wires. Only stainless steel, teflon and glass were allowed to come in contact with the water and all sealing was done with a silicone grease which does not contaminate water.

The thermal capacity of the foil assembly was sufficiently small that steady flow was attained within a few minutes. The large size of the tank made long test times, 30–40 min, possible without causing appreciable stratification or circulation in the tank. The temperature difference across the boundary region was usually of the order of 5–8 °F, permitting assumption of constant properties.

Constant-temperature hot-wire anemometers (Disa Model 55D01) were used to measure velocity. The longitudinal velocity was measured using only one hot wire with the sensor parallel to the vertical surface and perpendicular to the $x$ direction. Two wires in a V-arrangement were needed to measure the transverse velocity component. The sensor wire was platinum and 0·0005 in. in diameter while the hot-wire supports were silver plated. This configuration provides 'anodic protection' for the sensor as discussed by Hollasch & Gebhart (1972). The hot-wire overheat ratio used was 1·1. This resulted in a sensor temperature about 60 °F above the ambient. Since the temperature in the boundary region, except very close to the foil, was only a few degrees above the ambient, the error in velocity measurements due to temperature fluctuations and to background temperature changes was negligible. Calibration of the hot wires was carried out in water of resistivity of about 1 MΩ cm by the method of Dring & Gebhart (1969). For further details concerning calibration and velocity measurement, see Jaluria & Gebhart (1973).

The temperature measurements were made by means of a copper–constantan thermocouple 0·003 in. in diameter, using a reference temperature of 32 °F. This diameter gave a response time of the order of 8 ms. This was adequate for the frequencies encountered in this study. The thermocouple wires had a thin coat of nylon, for electrical insulation, which was removed at the ends to weld the junction. The thermocouple junction was located in the same horizontal plane as the hot wire. We found that the thermocouple reading was not disturbed by an active hot wire. The thermocouple wires were held in a pair of hollow glass tubes of diameter 0·05 in. These supporting tubes were attached to the support outside the boundary layer which also held the hot-wire probe. The location of the thermocouple junction with respect to the hot-wire sensor was accurately determined. The hot-wire and thermocouple signals were simultaneously recorded on a two-channel Offner Dynograph (type RS). At a sensitivity of 10 $\mu$V/cm, the temperature sensitivity was about 0·40 °F/cm.

The probe array could be positioned anywhere in the boundary region. The normal distance $y$ to the vertical surface was obtained from a micrometer with 0·001 in. divisions and the vertical ($x$) and transverse ($z$) positions using scales with divisions of 0·05 in. The exact location of the surface was determined by the electrical circuit described by Jaluria (1972).

Detailed local measurements were made over a wide range of the downstream location $x$ and surface heat flux $q''$. However, the basic procedure employed was to study the events for a wide range of $G^*$ at a given location $x$, by varying $q''$, before moving on to another location. This procedure was used in order to avoid frequent vertical repositioning of the probes and subsequent determination of the location of the surface. However, at each $x$, the same set of values of $q''$ was used. Thus, we obtained data for the downstream sequence of events for fixed values of $q''$. This corresponds to a single vertical surface studied at several different levels of heat flux.

All our experiments were carried out late at night to avoid the effect of large disturbances caused by the more intense daytime activity in the building. The mass and capacity of the tank further cushioned it from such disturbances. As

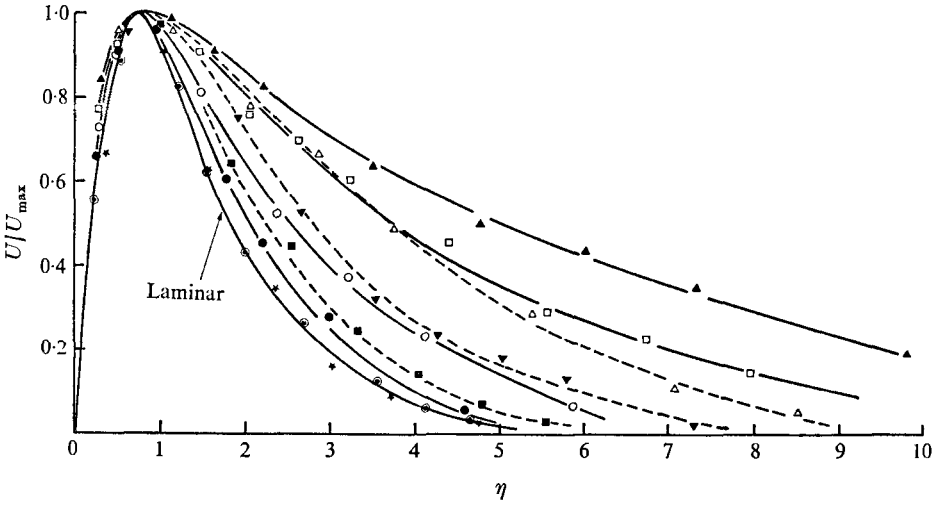


FIGURE 2. Mean velocity distribution. ——, $x$ = 42 in.; ⊙, $G^*$ = 752; ●, $G^*$ = 838; ○, $G^*$ = 914; □, $G^*$ = 1240; ▲, $G^*$ = 1342; – – – –, $x$ = 15 in.; ★, $G^*$ = 504; ■, $G^*$ = 551; ▼, $G^*$ = 586; △, $G^*$ = 625.

a check, many experiments were repeated on different nights to determine whether the results were altered. No significant variation was observed in our measurements and good reproducibility of data, within 5–10 % for the wall temperature, maximum velocity and surface heat flux, was found. We note that an error of 5–10 % in $q''$ gives rise to an experimental error of only 1–2 % in $G^*$ since $G^* \propto q''^{\frac{1}{5}}$.

## 3. Experimental results

### 3.1. *Mean velocity and temperature distributions*

An important aspect of the transition process is the change in the mean velocity and temperature distributions from laminar through transition to turbulent. We measured mean velocity and temperature profiles at various downstream locations $x$ and over a wide range of Grashof numbers $G^*$. At each location, measurements were first made in what was evidently locally completely laminar flow. The surface heat flux $q''$ was then increased in order to proceed through transition to complete turbulence at that location.

*Mean velocity profiles.* Distributions across the boundary region at $x$ = 15 and 42 in. and for the range of $G^*$ studied are shown in figure 2. The measured mean velocity $U$ is normalized by the maximum value $U_{\max}$ found in the traverse. The distance $y$ normal to the vertical surface is scaled as in laminar boundary-layer theory by $\delta = 5x/G^*$, to obtain the similarity variable $\eta = y/\delta$. These curves clearly show the changing form and extent of the velocity profile during transition. The laminar velocity profile calculated by Knowles (1967) for $Pr$ = 6·9 is shown for reference.

The data at $x$ = 15 in. for $G^*$ = 504 and at $x$ = 42 in. for $G^*$ = 752 are very close to the theoretical laminar profile. However, at $x$ = 15 in. for $G^*$ = 551 and

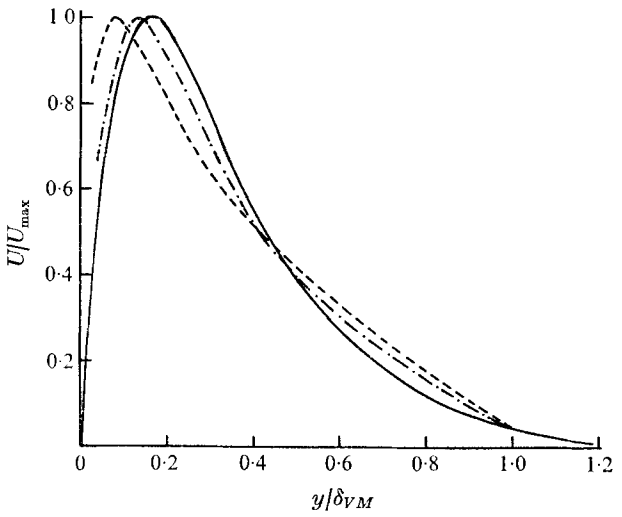


FIGURE 3. Mean velocity distribution $U/U_{max}$ *vs.* $y/\delta_{VM}$ at $x = 42$ in. ——, laminar, $G^* = 752$; –·–·–, $G^* = 914$; – – – –, $G^* = 1342$.

at $x = 42$ in. for $G^* = 838$ the profiles have become distorted and flow has been induced further out in the ambient medium. As the surface heat flux $q''$ is increased at each downstream location, the flow penetrates deeper into the ambient fluid as a consequence of growing turbulence in the boundary region. At $x = 42$ in. for $G^* = 1342$, the thickness of the boundary region is twice that of a laminar one. The downstream change in profile at a constant $q'' = 300$ B.Th.U/h ft$^2$ may be seen by comparing the results at $x = 15$ in. for $G^* = 551$ with those at $x = 42$ in. for $G^* = 1240$. We see a thickening of the boundary region and increased distortion.

An important point that emerges from the results in figure 2 is the dependence of the form of the profile on both the downstream location $x$ and on the value of $G^*$. For example, the mean velocity profile at $x = 42$ in. and $G^* = 752$ agrees closely with that for laminar flow, whereas at $x = 15$ in. and $G^* = 625$ we already have a pronounced distortion of the measured profile and considerable thickening of the boundary region. The similarity in the form of the curves at $x = 15$ in. for $G^* = 504$, 551 and 586 with those at $x = 42$ in. for $G^* = 752$, 838 and 914, respectively, also indicates that the mean velocity profile is not a function of $G^*$ alone but that it also depends strongly on the downstream location $x$, or on the surface heat flux $q''$. These results suggest that a correlating parameter should incorporate either $x$ or $q''$ with $G^*$.

The location (in $\eta$) of the maximum velocity remains approximately the same, at around $\eta = 0{\cdot}7$. The peak broadens with increasing $G^*$ and it becomes more difficult to determine its exact location. Nevertheless, our data show that the peak gradually shifts inwards, in terms of the physical distance $y$, as $G^*$ increases at a given location. It shifts outwards downstream at constant $q''$.

The changing form of the distributions is better seen when they are plotted, as in figure 3, against $y$ normalized by the measured local velocity boundary-layer

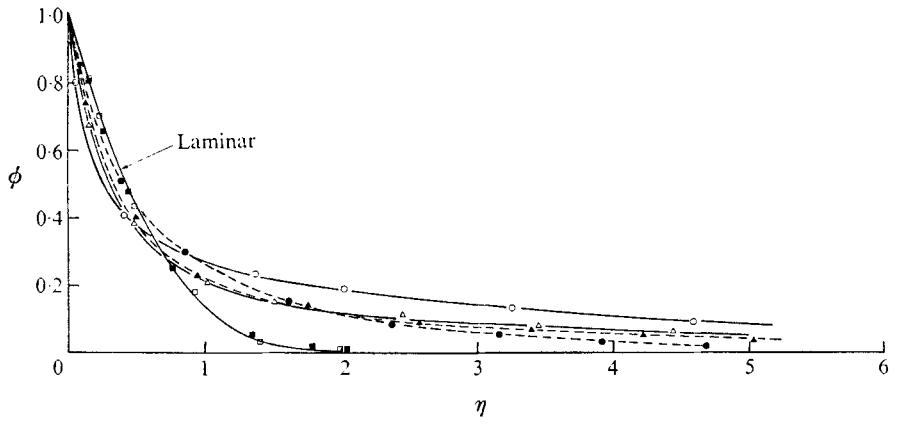


FIGURE 4. Mean temperature distribution. ——, $x$ = 42 in.; ■, $G^*$ = 914; △, $G^*$ = 1240; ○, $G^*$ = 1342; – – –, $x$ = 15 in.; □, $G^*$ = 551; ●, $G^*$ = 586; ▲, $G^*$ = 625.

thickness $\delta_{VM}$. Values of $\delta_{VM}$ were estimated from figure 2. However, the conventional definition of the edge of the boundary layer as the location (in $y$ or $\eta$) where the velocity has dropped to 1 % of its peak value was not practical. The profile in the outer portion of the boundary region is too flat. Therefore, the edge of the boundary layer was taken as the position at which the velocity had dropped to 5 % of its maximum value. A similar definition was later used for the thermal boundary-layer thickness $\delta_{TM}$.

Although figure 3 is a better correlation, there still remains systematic disagreement. The curves meet at $y/\delta_{VM} = 1$, by definition. Yet the peak is seen to shift towards the surface. Clearly no correlation may be obtained by scaling $y$ in any way. Efforts of Cheesewright (1968) and Vliet & Liu (1969) to obtain such a correlation in turbulent flow did not yield any satisfactory result. The forms of our distributions agree with theirs in the shift of the peak towards the surface and a flattening of the profile near the inflexion region with increasing $G^*$.

*Mean temperature profiles.* These distributions are plotted in figure 4. The results are in terms of $\phi = (T - T_\infty)/(T_0 - T_\infty)$ *vs.* $\eta$, where $T$ is the local fluid temperature, $T_0$ is the local surface temperature and $T_\infty$ is the temperature of the ambient medium. $T_0$ was determined by extrapolation of the measurements of mean temperature to the surface. This value was found to be slightly less than the theoretical value in the laminar regime and it decreased during transition, as observed by Vliet & Liu (1969) and discussed in more detail later.

At $x$ = 15 in. for $G^*$ = 551 and at $x$ = 42 in. for $G^*$ = 914 the measured profiles agree closely with the laminar profile, also calculated by Knowles (1967). With increasing $G^*$ the profiles steepen near the surface and flatten at higher $\eta$. The thermal boundary region thickens as $G^*$ increases. At $x$ = 42 in. for $G^*$ = 1342, the thickness of the boundary region is about four times that of a laminar one. The general form of these curves agrees with the measurements made by Godaux & Gebhart (1974), Cheesewright (1968) and Warner (1966) in the transition regime. Such thickening is expected to follow the thickening of the velocity region. As the flow penetrates deeper into the ambient medium it also diffuses

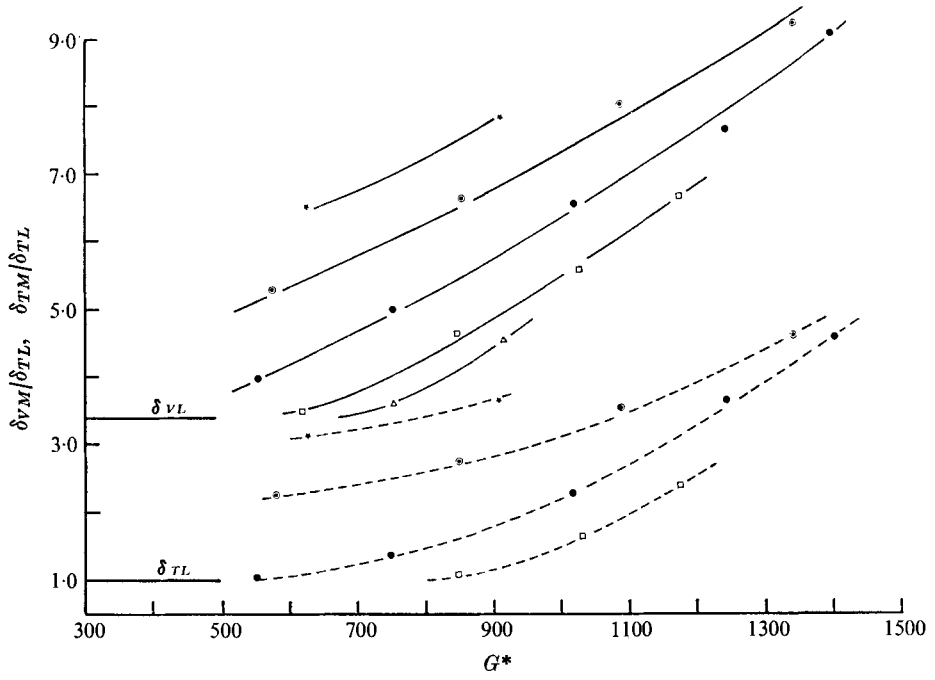


FIGURE 5. Downstream growth of boundary-layer thickness with $G^*$ for various values of $q''$ (in B.Th.U./h ft$^2$). ——, velocity; – – –, temperature; △, $q'' = 67$; □, $q'' = 120$; ●, $q'' = 300$; ⊙, $q'' = 415$; ★, $q'' = 595$.

the warm fluid outward. The temperature and velocity field are linked and, depending on the magnitude and size of the turbulent eddies, the thermal boundary region diffuses further into the ambient medium.

These results show that the progression of thermal transition also does not depend on $G^*$ alone. At $x = 15$ in. the distribution for $G^* = 625$ is greatly distorted from laminar form whereas at $x = 42$ in. for the higher value $G^* = 914$, it is just beginning to deviate. The flow has progressed well into transition at $G^* = 625$ even before the beginning of distortion at $G^* = 914$, at a lower value of $q''$. Clearly $\eta$ does not correlate these mean temperature profiles. Nor would a normalization of $y$ by the measured thermal boundary-layer thickness $\delta_{TM}$.

*Growth of boundary-layer thickness.* The measured growth of $\delta_{VM}$ and $\delta_{TM}$ with $G^*$ is shown in figure 5 for several values of the surface heat flux $q''$. Both were normalized by the theoretical thermal boundary-layer thickness $\delta_{TL}$ for laminar flow. With our definition (5 %) of boundary-layer thickness, $\delta_{TL} = 1{\cdot}35\delta$. Both boundary-layer thicknesses are seen to increase with transition from the laminar values of 1·0 and 3·3. The location of the deviation depends sharply on the value of $q''$. However, the rate of growth with $G^*$ is not sharply dependent on $q''$, although the rate of growth with $x$ increases at higher $q''$, since $G^* \propto (q''x^4)^{\frac{1}{5}}$. Since $\delta_{VM}$ begins to deviate from the laminar value at a lower $G^*$ than does $\delta_{TM}$, the flow field is seen to be the key to the transition mechanism. This is not surprising, given the disparate boundary-region thicknesses at this Prandtl number.

We also infer from figure 5 that the ratio $\delta_{VM}/\delta_{TM}$ decreases with $G^*$, for

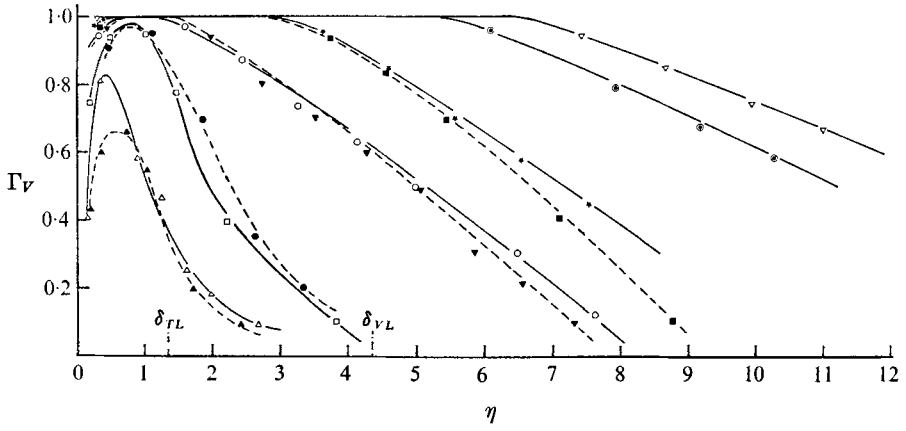


FIGURE 6. Variation of the velocity intermittency factor $\Gamma_V$ across the boundary region. ——, $x$ = 42 in.; △, $G^*$ = 752; □, $G^*$ = 838; ○, $G^*$ = 914; ★, $G^*$ = 1028; ⊙, $G^*$ = 1240; ▽, $G^*$ = 1342; ----, $x$ = 15 in.; ▲, $G^*$ = 504; ●, $G^*$ = 551; ▼, $G^*$ = 586; ■, $G^*$ = 625.

a given $q''$. For example, for $q''$ = 300 B.Th.U./h ft$^2$, this ratio decreases from 4·0 to 1·9 as $G^*$ increases from 550 to 1400. Thus, after its initial deviation, the thermal boundary-layer thickness grows more rapidly. This is presumably due to the growth of velocity turbulence to a large enough scale to cause very rapid mixing of the thermal boundary-layer material.

Even though the thickness of the thermal boundary region rapidly increases, it never equals the velocity-region thickness. The measurements of Vliet & Liu (1969) in fully turbulent flow indicate that $\delta_{VM}/\delta_{TM}$ becomes about 2·0, according to our definition of boundary-layer thickness. We find about 1·9.

### 3.2. *The growth of turbulence*

The measured progress of transition, from the first appearance of turbulent bursts to complete turbulence, is presented in terms of the local intermittency factor $\Gamma(x, y)$ defined earlier. Distributions of $\Gamma(x, y)$ across the boundary region indicate turbulence growth with $G^*$ and the end of transition may be inferred from their characteristics.

Distributions of the velocity intermittency factor $\Gamma_V$ at the two locations $x$ = 15 and 42 in. for various $q''$ are shown in figure 6. At both locations, for the smallest values of $G^*$ the curves are seen to be very narrow and extend out only to about $\eta = 3$. The flow beyond is still entirely laminar. The maxima in the distributions at $x$ = 15 in. for $G^*$ = 504 and at $x$ = 42 in. for $G^*$ = 752 are at around $\eta$ = 0·8 and are, thus, close to the maxima of the mean velocity profiles, which, as we have seen, have not as yet deviated from the laminar ones.

With increasing $G^*$, the $\Gamma_V$ distributions quickly reach further out in $\eta$. The maximum value also rises to $\Gamma_V = 1$, i.e. to complete local turbulence. The region of complete local turbulence also grows. At $x$ = 42 in. and $G^*$ = 1342 the boundary region is completely turbulent out to $\eta$ = 6·5. Although $\Gamma_V$ decreases gradually beyond this, the flow is turbulent more than half the time even at $\eta = 12$.

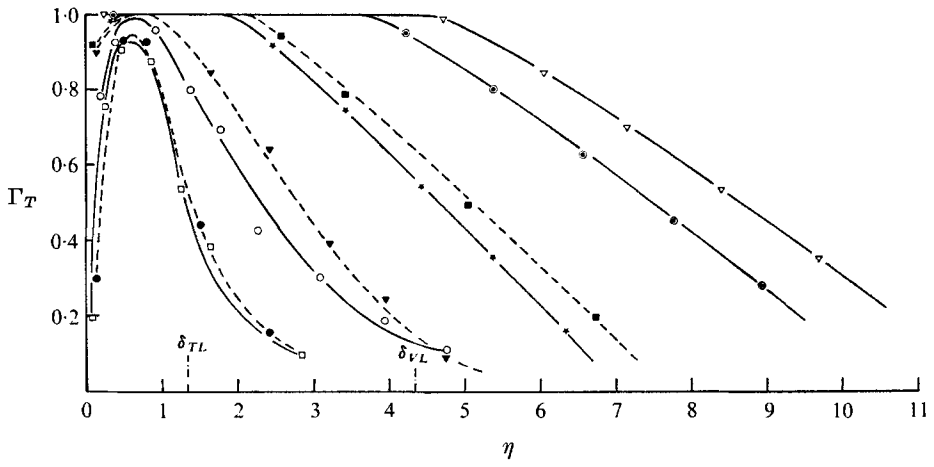


FIGURE 7. Variation of the thermal intermittency factor $\Gamma_T$ across the boundary region. ——, $x = 42$ in.; □, $G^* = 838$; ○, $G^* = 914$; ★, $G^* = 1028$; ⊙, $G^* = 1240$; ▽, $G^* = 1342$; ----, $x = 15$ in.; ●, $G^* = 551$; ▼, $G^* = 586$; ■, $G^* = 625$.

Figure 6 indicates a steep decrease in $\Gamma_V$ in the immediate vicinity of the surface. This is particularly apparent at smaller values of $G^*$. Thus the flow close to the surface is predominantly laminar. This is probably due to damping at the wall. Lock & de B. Trotter (1968) did not find this laminarization near the surface, although they did measure a damping effect on disturbance amplitude there. Since they used tap water, presumably of low resistivity, leakage currents to the surface might have caused considerable errors in the readings.

The changing $\Gamma_V$ distributions are consistent with the change in the mean velocity profiles in figure 2. The expansion of the flow field out into the ambient medium accompanies spreading $\Gamma_V$ distributions. Apparently the initial turbulent eddies are small and weak. However, as they are convected downstream they grow in size and in strength and more effectively mix fluid across the boundary region, giving rise to the broad $\Gamma_V$ curves at higher $G^*$.

Corresponding distributions of the temperature intermittency factor $\Gamma_T$ are plotted in figure 7. Their behaviour is similar. Highly localized turbulence in the temperature field, evident from the narrow distribution, which also peaks at around $\eta = 0{\cdot}8$, spreads outward in the velocity boundary region as $G^*$ increases. Again the region nearest the surface is predominantly laminar.

A comparison of the $\Gamma_T$ and $\Gamma_V$ distributions indicates another significant feature of these flows, that is, that turbulence appears first as velocity disturbances and only further downstream as thermal disturbances. Although turbulence was observed in velocity at $x = 15$ in. for $G^* = 504$ and at $x = 42$ in. for $G^* = 752$ (see figure 6), no turbulence is found in temperature. Figures 6 and 7 also indicate that the $\Gamma_V$ distributions spread out further in the boundary region than do those of $\Gamma_T$. Compare, for example, the results at $x = 42$ in. and $G^* = 914$. Thus the temperature disturbances follow the velocity disturbances. As turbulent eddies grow, greater mixing in the boundary region causes the turbulent thickening of the thermal region. Later investigations of both the

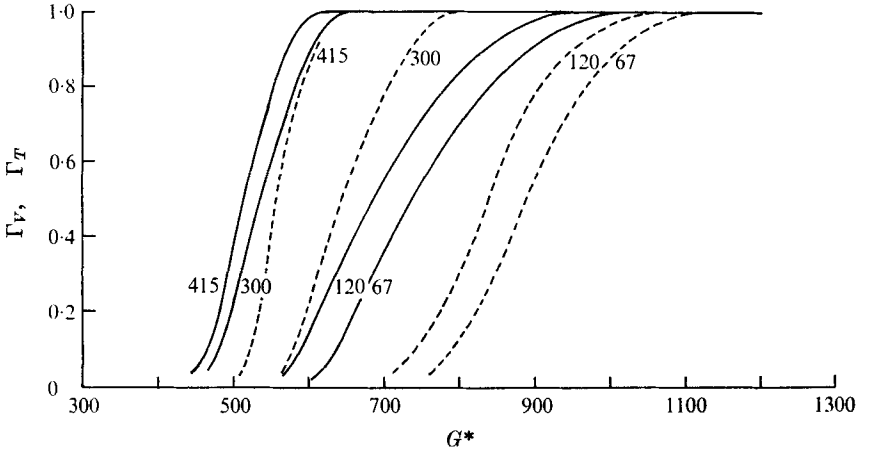


FIGURE 8. Variation of the intermittency factors $\Gamma_V$ and $\Gamma_T$ with $G^*$ at $\eta = 2$. ——, velocity; – – – –, temperature. The numbers shown on the curves indicate the value of $q''$ in B.Th.U./h ft$^2$.

frequency and growth of velocity and temperature disturbances offer additional evidence for these conclusions.

The rate of downstream development of turbulence may perhaps be seen more clearly by plotting $\Gamma$, at $\eta = 2$, *vs.* $G^*$ for various values of $q''$, as shown in figure 8. The growth from the first appearance of bursts is seen to be very rapid. These curves clearly indicate that for any given $q''$, that is, given uniform surface flux, the turbulence arises first in the velocity field. Although $\Gamma_T$ deviates from zero after $\Gamma_V$, it increases more rapidly to complete turbulence downstream.

These $\Gamma$ curves are strongly dependent on $q''$. At higher values both initial transition and complete turbulence occur at smaller $G^*$. We again see the independent importance of $q''$ in the range of $G^*$ corresponding to transition.

### 3.3. *The end of transition*

With this increased understanding of the progress of transition we now consider the definition of the end of transition, as distinct from the onset of 'developed' turbulence yet further downstream. We shall see later that this additional process must be of fundamental importance in this flow. The end of transition should be taken as the end of the downstream variation of some quantity characteristic of transition. Cheesewright (1968) defined it as the downstream location where major changes in the form of the mean temperature profiles ended. One might also choose the location where the ratio $\delta_{VM}/\delta_{TM}$ reaches a constant value. However, such criteria are neither sharply defined nor accurately measurable.

The growth of turbulence is characterized by $\Gamma$ and it would perhaps be physically reasonable to define the end of transition in these terms. We could choose the downstream location where the flow at an arbitrary value of $\eta$ becomes completely turbulent. However, the boundary region thickens with $G^*$ and the region of complete turbulence continues to expand. Choosing an arbitrary $\eta$ location, without giving due consideration to the thickness $\delta_{VM}$ or $\delta_{TM}$, would not be reasonable and would not uniquely characterize the end of transition.

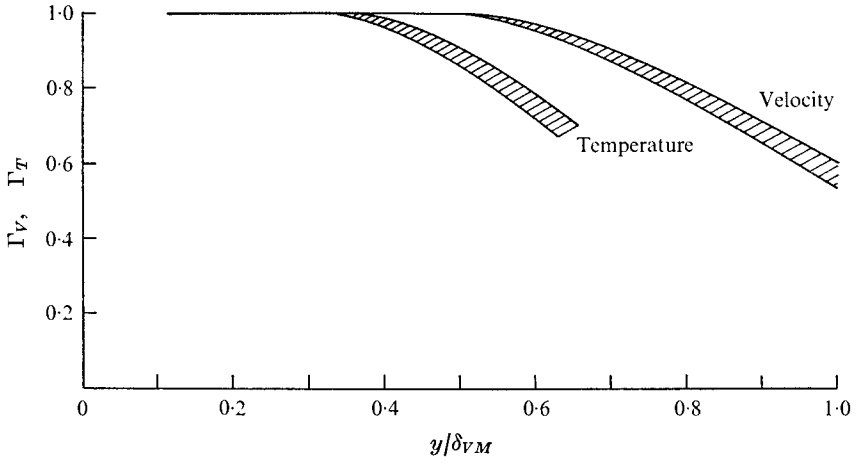


FIGURE 9. Distribution of the intermittency factors $\Gamma_V$ and $\Gamma_T$ across the boundary region at the end of transition for the downstream locations $x$ where measurements were taken.

The criterion we propose here was first applied separately to the velocity and to the temperature field, in order to determine whether the resulting downstream location of the end of transition was the same by the two measures. These criteria were defined in terms of the distributions of $\Gamma_V$ and $\Gamma_T$ *vs.* $y$ normalized by $\delta_{VM}$ and $\delta_{TM}$, respectively. We recall that the distributions of $\Gamma_V$ and $\Gamma_T$ spread out with increasing $G^*$. However, it might be true that, beyond the end of transition, their form does not continue to change, in terms of $y/\delta_{VM}$ and $y/\delta_{TM}$. This amounts to looking for a correlation in terms of $y/\delta_{VM}$ and/or $y/\delta_{TM}$.

We found that the values of both $\Gamma_V$ and $\Gamma_T$ at the measured edge of the boundary region initially increase rapidly with $G^*$ during transition. They then reach a more or less fixed value. The value of $G^*$ at which this occurs was taken as the end of transition. Intermittency was also found to correlate well downstream in terms of $y/\delta_{VM}$ and/or $y/\delta_{TM}$. Though our criterion is probably not as sharply defined as is the first appearance of bursts at the beginning of transition, we found that we could still apply it accurately if sufficient data were available in the region close to the end of transition. Finally, applying this criterion separately to $\Gamma_V$ and $\Gamma_T$, we found that the end of transition was attained at the same downstream location, or $G^*$, for any given value of $q''$.

Clearly, the end of the transition regime signifies the end of a progressive process, and, as such, this end cannot be distinctly specified in terms of a definite value of $G^*$ nor defined uniquely. However, in order to determine the effect of $q''$ on the end of transition it is necessary to use a measure which is relatively sharp and reliable. The distributions of $\Gamma$ have these characteristics.

Another interesting observation about the end of transition is apparent in a plot of both the $\Gamma_V$ and $\Gamma_T$ distributions there *vs.* $y/\delta_{VM}$. These are shown in figure 9 for downstream locations $x = 24$, 33, 42 and 48 in. with $G^* = 910$, 1083, 1240 and 1320. The respective distributions fall within the two narrow shaded regions. Thus, at the end of transition at various values of $q''$ the $\Gamma$ *vs.* $y/\delta_{VM}$ curves are very similar. This suggests a turbulence structure at the beginning of complete turbulence which is in some way independent of $q''$.

The measured limits of the transition regime are plotted in figure 16 in terms of $G^*$ and $q''$. Linear trends are found for both the beginning and end of the transition regime on a log–log scale. Transition is seen to begin and end at lower $G^*$ for higher $q''$. Also shown are the limitations of our experiments since $x \leqslant 52$ in. and $q'' \leqslant 700$ B.Th.U./h ft$^2$. We were able to study the complete process only in a narrow range of $q''$. The curves indicate that a parameter of the form $G^*q''^m$, or $G^*x^{-n}$, characterizes the limits of transition. We shall later determine $m$ and $n$ and discuss the possible physical significance of these quantities.

### 3.4. *The frequency of disturbances*

We know from earlier investigations of laminar instability (see Gebhart 1969, 1973) that these boundary-layer flows amplify input frequencies selectively and over a very narrow band of frequencies. It is important to an understanding of the origin and growth of bursts to know whether such a concentration of disturbance energy into almost a single frequency continues into the transition processes. We also wish to know how any principal disturbance frequency survives and changes through transition to complete turbulence.

A detailed study of the frequency of both velocity and temperature disturbances was carried out at various $x$ and $q''$ during transition. In any single experimental recording of fluctuations, i.e. at a given $x$ and $y$, we found that almost a single 'predominant' frequency dominated the turbulent portion of the record and that another significantly lower 'principal' frequency dominated the laminar portion. Approximately 10 measurements were made of each of these frequencies, at each condition, and averaged as either the predominant or principal frequency. Although the data we report here were taken at around $\eta = 1$, each of the two characteristic frequencies was essentially constant across the boundary region, for given $x$ and $q''$.

It would have been desirable to analyse the disturbance frequency spectrum and to determine accurately these dominant frequencies. However, this is a very difficult undertaking, for which we were not prepared. We know of no proven analog instrumentation for detailed spectrum analysis below 1 Hz. The use of a Fourier transform method on digitalized data appears promising but we have not yet been able to determine to our satisfaction that available amplifiers and analog-to-digital converters, coupled to digital tape, offer both stability and suitably low signature at these frequency levels.

The frequency of the most-amplified disturbance at a given $G^*$ is predicted by linear stability analysis in terms of the generalized frequency $\beta$, where $\beta = (25x^2/\nu G^{*3})\, 2\pi f$ and $f$ is the physical frequency. This is rewritten as $f = C\beta G^{*\frac{1}{2}} q''^{\frac{1}{2}}$, where $C = (2\pi)^{-1}(g\beta_T/k)^{\frac{1}{2}}$. Now $\beta$ for the most-amplified disturbance is only a function of $G^*$. Therefore, $f/Cq''^{\frac{1}{2}}$ is a non-dimensional function of only $G^*$; it is independent of $q''$ and $x$. We have plotted the downstream variation of the dominant disturbance frequencies in this form in figure 10, for several values of $q''$. The relation obtained from linear stability analysis by Hieber & Gebhart (1971), for our experimental conditions, is also shown.

Data at the same $q''$ levels are fitted with curves. Clearly the laminar or principal frequency data agree very closely with the predictions of the linear

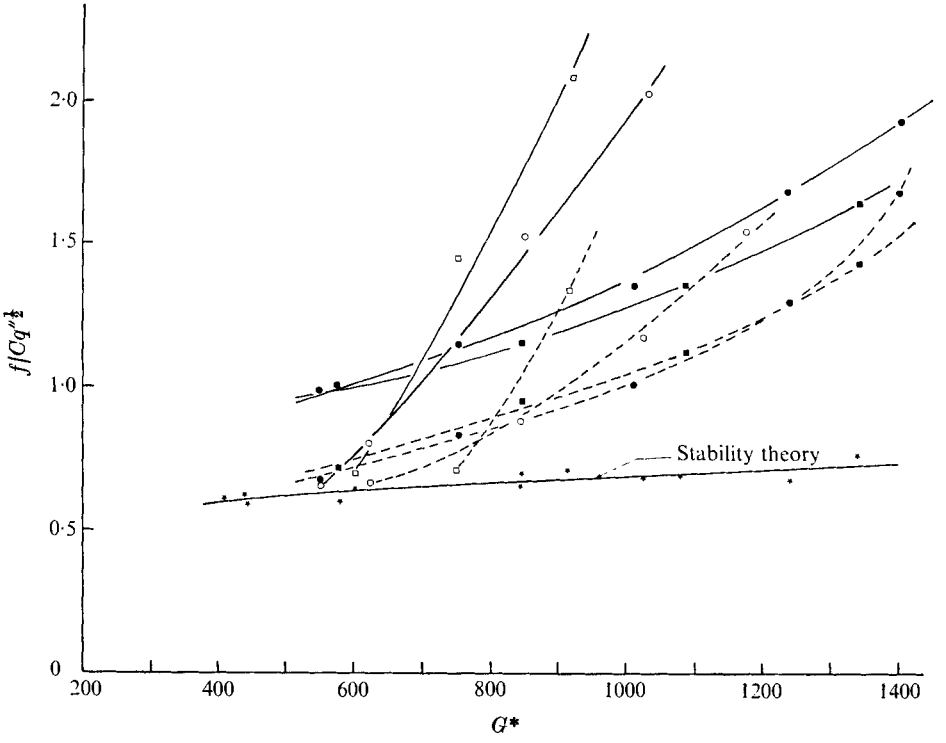


FIGURE 10. Variation of the dominant turbulent disturbance frequency, velocity and temperature, with $G^*$. ——, velocity; – – –, temperature; □, $q'' = 67$ B.Th.U./h ft$^2$; ○, $q'' = 120$; ●, $q'' = 300$; ■, $q'' = 415$; ★, during locally laminar flow.

theory, thereby lending strong support to both our measurements and to the predictions of theory. However, the predominant frequency, in periods of turbulence, is seen to be progressively greater than the corresponding laminar value. It also increases rapidly during transition. The level and slope of the curves depend strongly on the value of $q''$. Transition is again implied by these data to begin at a lower $G^*$ for larger $q''$. The rate of increase of $f/Cq''^{\frac{1}{2}}$ with $G^*$ is lower at higher $q''$. However, the rate of increase of the physical frequency $f$ with $G^*$ was found to be approximately independent of $q''$. We point out, incidentally, that the expected accuracy of these frequency determinations decreases through transition as both the velocity and temperature disturbances are progressively distorted from their almost purely sinusoidal form at the beginning of transition.

Another very important property of these data is that the local predominant frequency of the temperature disturbance is less than that of the velocity disturbance, at all values of $q''$. This would be anticipated from the earlier finding of delayed thermal transition. The predominant frequency of the velocity disturbance increases downstream. Temperature disturbances are produced by those in the velocity field. Since their detection depends upon the turbulent eddy size being sufficiently large to be measurable, the increase in frequency is seen further downstream. The temperature disturbance frequency never quite catches up during transition.

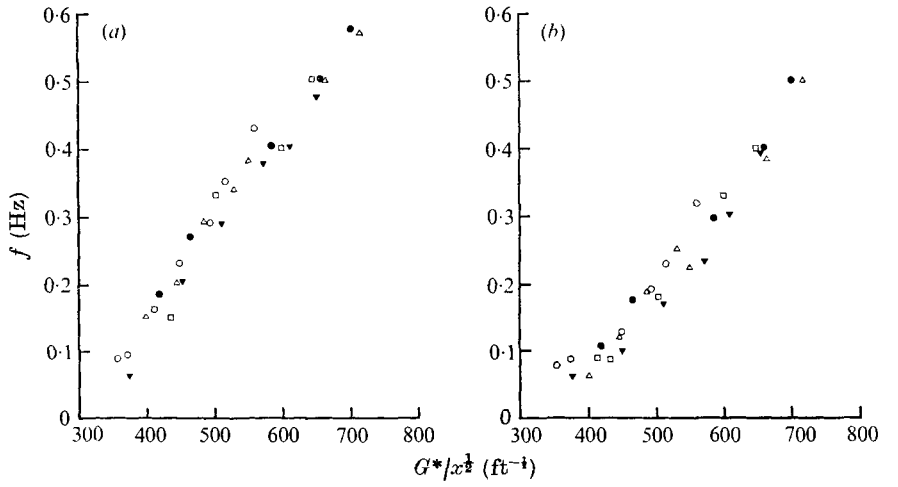


FIGURE 11. Variation of the principal turbulent disturbance frequency with $G^*/x^{\frac{1}{2}}$. The three points on the extreme left are for laminar flow. ○, $x = 15$ in.; □, $x = 24$ in.; ▼, $x = 33$ in.; △, $x = 42$ in.; ●, $x = 48$ in. (*a*) Velocity. (*b*) Temperature.

We may approximately correlate the turbulent frequency data of figure 10 for both velocity and temperature by using $G^*/x^{\frac{1}{2}}$ instead of $G^*$, as shown in figure 11 for $x = 15, 24, 33, 42$ and 48 in. This correlation indicates the importance of a parameter of the form $G^*/x^n$. Some data for the principal laminar frequency near the beginning of transition also follow the same trend. These correlations emphasize that the frequency of temperature disturbances is lower than those of the velocity disturbances.

### 3.5. *Disturbance growth during transition*

We also measured the downstream growth of the maximum amplitude of both the velocity and temperature disturbances to compare their growth rates, to determine any dependence on $q''$ and to compare their growth rates with those predicted by linear theory. Figure 12 shows the results for $q'' = 67$ B.Th.U./h ft$^2$. The measured local maximum amplitude across the boundary region at each $x$ is normalized by that measured at $G^* = 400$. The curve predicted by linear stability theory (Hieber & Gebhart 1971) is also drawn.

The measured growth rate initially follows the predicted one until at around $G^* = 430$ it becomes greater. This agrees qualitatively with the results of the experimental study of Jaluria & Gebhart (1973), with controlled disturbances, in which it was found that nonlinear mechanisms led to a higher growth rate from about $G^* = 400$ to 550. The actual growth rate then quickly begins to decrease and becomes less than that predicted beyond about $G^* = 570$. At large disturbance amplitude these other mechanisms clearly compete for disturbance energy. Transition begins at $G^* = 630$. Further downstream the maximum disturbance amplitude in the boundary region was found to occur during times of local turbulence.

Growth rates measured for $q'' = 200$, 300 and 415 B.Th.U./h ft$^2$ are shown in figure 13 for the $G^*$ range 600–1400. Transition begins further upstream for these

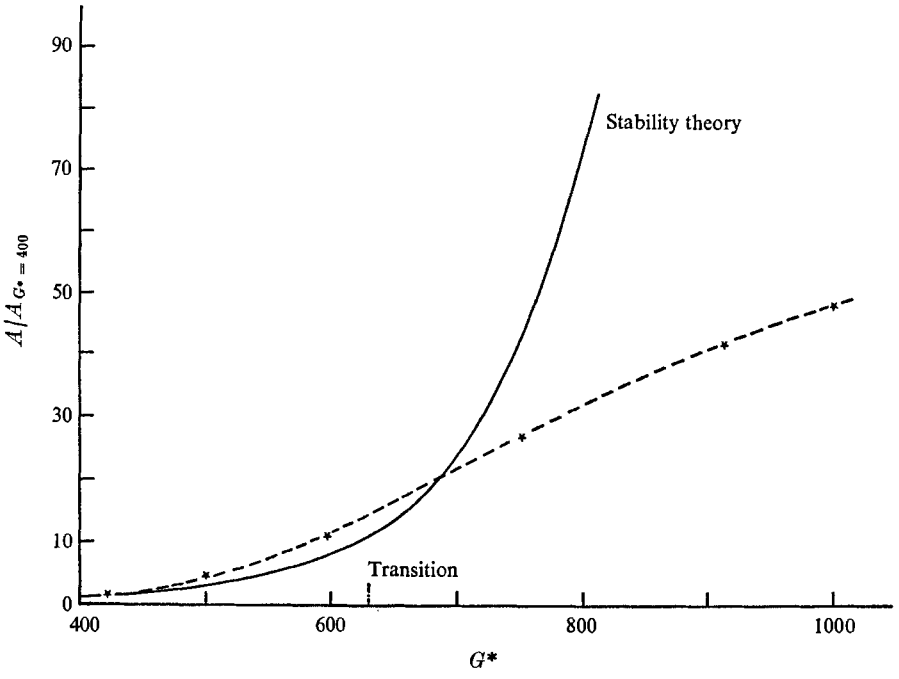


FIGURE 12. Downstream amplification of velocity disturbance $u'$ with $G^*$ at $q'' = 67$ B.Th.U./h ft$^2$.

values of $q''$ and the curves show disturbance growth during transition. All amplitudes are normalized by the values measured at $G^* = 600$ for $q'' = 200$ B.Th.U./h ft$^2$, chosen because they are the lowest amplitudes measured. The local disturbance amplitude at $G^* = 600$ increases with $q''$, indicating that disturbances have grown faster at higher $q''$ up to $G^* = 600$. We see that the fractional increase in disturbance amplitude above $G^* = 600$ decreases with $q''$. Recall that these amplitudes were measured in the transition region. Perhaps the increasing dominance of turbulent transport mechanisms in the diffusion of concentrated disturbance energy has already occurred.

We also note a lower growth rate of temperature disturbances. This is again the cause-and-effect link between velocity and the temperature fields. Although initially there is a substantial difference in the two growth rates, they become nearly equal at higher $G^*$.

### 3.6. *Disturbance amplitude distributions across the boundary region*

Measured local maximum velocity and temperature disturbance amplitude distributions (in $\eta$) are shown for $q'' = 415$ B.Th.U./h ft$^2$ in figures 14 ($a$) and ($b$) respectively. The transition region lies between $G^* = 450$ and 1100 at this value of $q''$. Each distribution is normalized by the maximum amplitude measured across the boundary region. The prediction from stability analysis by Dring & Gebhart (1968), for $G^* = 300$ and the most-amplified disturbance frequency, is also shown.

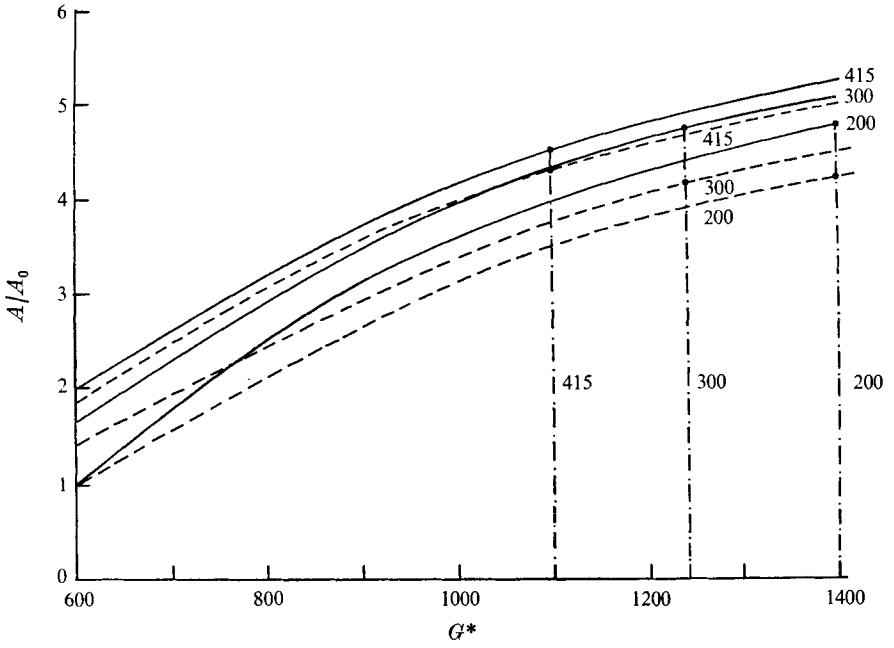


FIGURE 13. Downstream amplification of velocity and temperature disturbance. $A_0$ is the disturbance amplitude at $G^* = 600$ for $q'' = 200$ B.Th.U./h ft$^2$. The numbers shown on the curves indicate the value of $q''$. ——, velocity; – – –, temperature; –·–, end of transition.

The velocity data have two maxima, as does the theoretical curve. The inside peaks are also close to the calculated one and shift towards the wall with increasing $G^*$. Similar behaviour was observed by Vliet & Liu (1969). The outer peak moves outwards with increasing $G^*$, as velocity disturbances spread out from the surface. However, the distribution at $G^* = 1342$ shows an anomalous behaviour. The velocity disturbance has spread out further in $\eta$ than at $G^* = 1083$, as expected from the growth of the boundary-region thickness. But the distribution is much flatter in the outer portion of the boundary region and the outer peak value in the distribution is unexpectedly lower. We recall that this transition ends at $G^* = 1100$. This unexpected change in the distribution from $G^* = 1083$ to $G^* = 1342$ may perhaps be related to the rapidly growing eddy size, discussed subsequently. Larger disturbances encounter the lower velocity fluid near the ambient condition more abruptly, which would tend increasingly to damp them.

The temperature disturbance data in figure 14(*b*) show a somewhat similar behaviour, although there is only one peak, similar to the theoretical result. Again, the peak moves towards the surface with increasing $G^*$, in agreement with the observations of Godaux & Gebhart (1974). The temperature disturbances penetrate further out with increasing $G^*$. The distribution at $G^* = 1342$ again shows an anomaly.

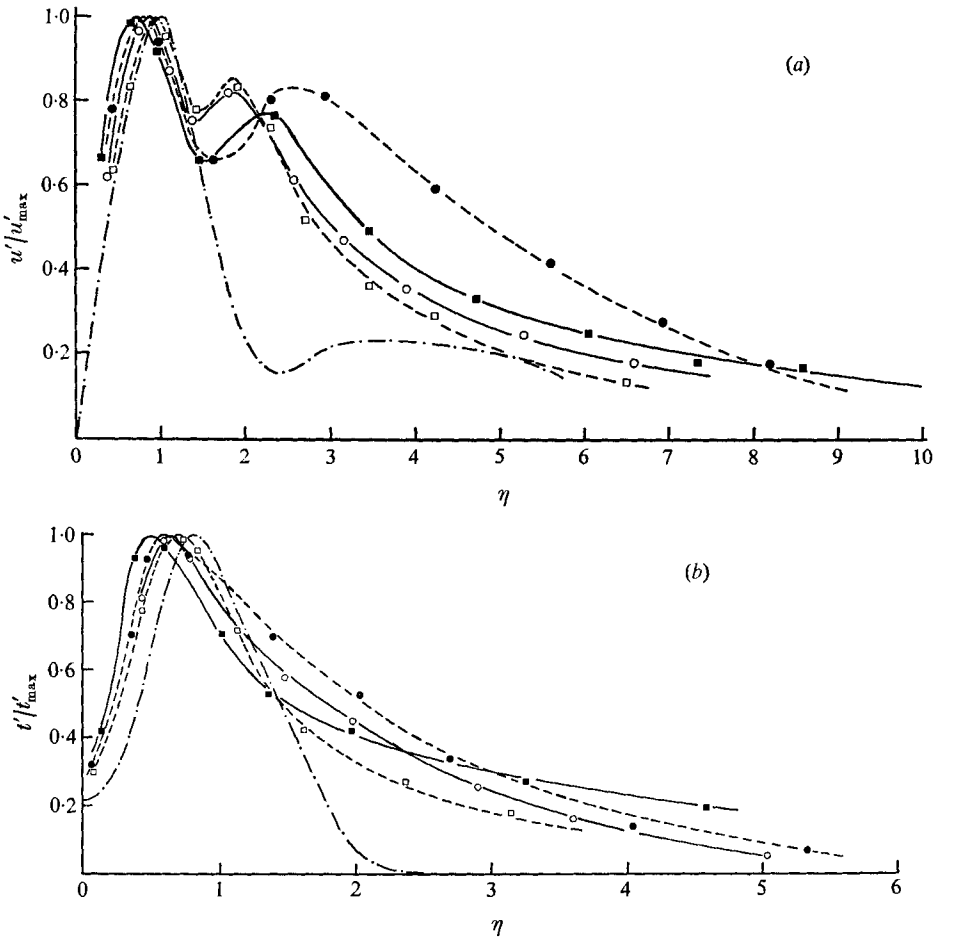


FIGURE 14. Variation of the amplitude of (*a*) the velocity disturbance $u'$ and (*b*) the temperature disturbance $t'$ across the boundary region at $q'' = 415$ B.Th.U./h ft$^2$. –·–·–, disturbance profile calculated by Dring & Gebhart (1968) at $G^* = 300$ for highly amplified disturbance. Present data: □, $G^* = 586$; ○, $G^* = 847$; ●, $G^* = 1083$; ■, $G^* = 1342$.

### 3.7. *Disturbance level in the boundary region*

We also studied the downstream variation of the disturbance level in the boundary region to obtain further information on changes in boundary-layer structure during transition. The results are plotted in figure 15 (*a*) as the maximum amplitudes $u'$ and $t'$ across the boundary region of the velocity and temperature disturbances at a given $G^*$ normalized by the local measured maximum mean velocity $U_{max}$ and the local temperature difference $\Delta T$ across the boundary region, respectively. Distributions of $U_{max}$ normalized by $\nu/x$ and of $\Delta T$ normalized by the local temperature difference $\Delta T_L$ calculated for laminar flow, as indicated in the appendix, are shown in figure 15 (*b*). These data are for $q'' = 300$ and 415 B.Th.U./h ft$^2$.

First, from figure 15 (*b*) we see that the measured maximum mean velocity is always less than that calculated for laminar flow and increasingly so downstream.

For $q'' = 300$ B.Th.U./h ft$^2$, the difference increases from 15 % to 30 % from $G^* = 550$ to 1500. The data for $q'' = 415$ B.Th.U./h ft$^2$ show somewhat less deviation. The maximum mean velocity measured by Jaluria (1972) in laminar flow was found to be about 10 % less than the calculated one.

The measured wall temperature $\Delta T/\Delta T_L$ is also less than the theoretical value for laminar flow, i.e. 1·0. The difference increases from 15 % to 64 % for $q'' = 300$ B.Th.U./h ft$^2$ as $G^*$ increases from 550 to 1500. At the higher $q''$ value the deviation is greater in spite of the measured value of $\Delta T$ being greater at the higher $q''$. The wall temperature ratio decreases during transition and then approaches a constant value as transition is completed. This trend agrees with the wall temperature measurements of Vliet & Liu (1969).

Since the disturbance quantities $u'$ and $t'$ are normalized in figure 15(*a*) by the corresponding measured maximum mean value, we see that the disturbance amplitudes quickly become comparable with the mean flow quantities. The peak value of $u'$ is 50 % and that of $t'$ is 75 %. Maximum values occur near the end of transition. These disturbance magnitudes are relatively very large and much greater than those found in forced boundary-layer flows.

This downstream variation of amplitude during transition has very interesting implications. Temperature disturbance growth appears complete by the end of transition. However, velocity disturbances have already passed their maximum relative values. These changes perhaps signal a further decrease in the size and intensity of turbulent eddies. This behaviour is somewhat similar to that observed by Klebanoff, Tidstrom & Sargent (1962) in forced flow, but at a much lower intensity level.

### 3.8. *Transverse flow*

We also measured the transverse component $W$ of the mean velocity and the amplitude $w'$ of the fluctuating component to find whether our results in a flow subject only to natural disturbances agree with those obtained by Jaluria & Gebhart (1973) under controlled conditions in laminar flow and those calculated by Audunson & Gebhart (1975) with nonlinear disturbance growth mechanisms. The measurements were made at $G^* = 570$ for $q'' = 67$ B.Th.U./h ft$^2$. This location is just upstream of the beginning of transition; see figure 12. Data taken from $\eta = 1{\cdot}0$ to 2·0 indicated the presence of both $W$ and $w'$. $W$ was found to vary with $\eta$ with a local maximum around $\eta = 1{\cdot}5$. The maximum value of $W/U_{\max}$ found by Jaluria & Gebhart (1973) was around 0·06. However, we found about 0·005. Klebanoff *et al.* (1962) also found a similar sharp drop in the value of $W$ between flows subject to controlled disturbances and those with only natural disturbances.

The small magnitude of $W$ and $w'$ made it impossible to obtain reliable results close to the wall and in the outer portion of the boundary region, because of background noise in the hot-wire output. Thus, the complete variation of $W$ across the boundary region was not obtained. However, the presence of $W$ and its variation over a portion of the boundary region imply longitudinal rolls similar to those predicted by the analysis and also measured. At a lower value of $q''$ and at the same location, $W$ could not be detected over the noise. This is in accordance with an expectation of increased nonlinear effects and vortical motion at higher

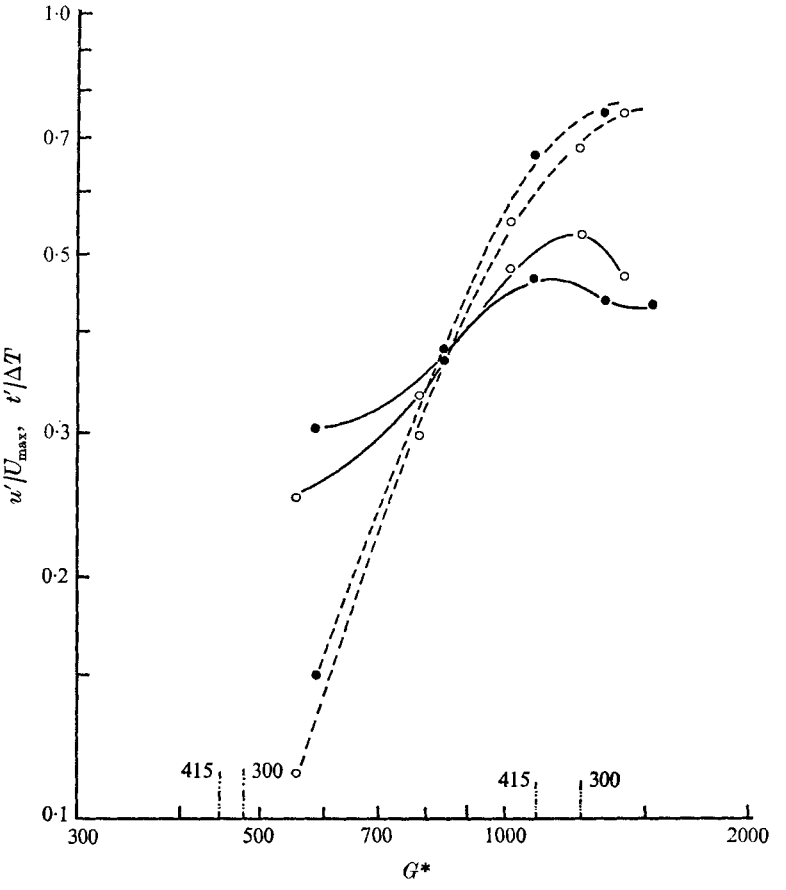


FIGURE 15 (*a*). For legend see facing page.

$G^*$. All of our measurements of $w'$ showed it to be almost sinusoidal with a frequency close to that of $u'$, which also agrees with the implications of stability analysis.

## 4. Transition criteria

Our results show in many ways that the Grashof number $G^*$ does not correlate the events of transition. Either $x$ or $q''$ must be considered along with $G^*$. This is perhaps most clearly seen in figure 16, where the measured $G^*$ limits of the transition regime are plotted against $q''$. These limits lie at lower $G^*$ for higher $q''$. Our measurements of mean velocity, mean temperature and of the intermittency factor $\Gamma(x, y)$ suggested a correlation parameter of the form $G^*/x^n$. Figure 16 indicates that each transition limit varies linearly with a negative power of $q''$, indicating a parameter of the form $G^*q''^m$, or $G^*/x^n$, which is equivalent. The value of $m$ is about 0·2 for the beginning of both velocity and thermal transition and that of $n$ is about 0·4. At the end of transition, $m \simeq 0{\cdot}41$ and $n \simeq 0{\cdot}54$.

The importance of $G^*$ as the correlating parameter is suggested by tradition

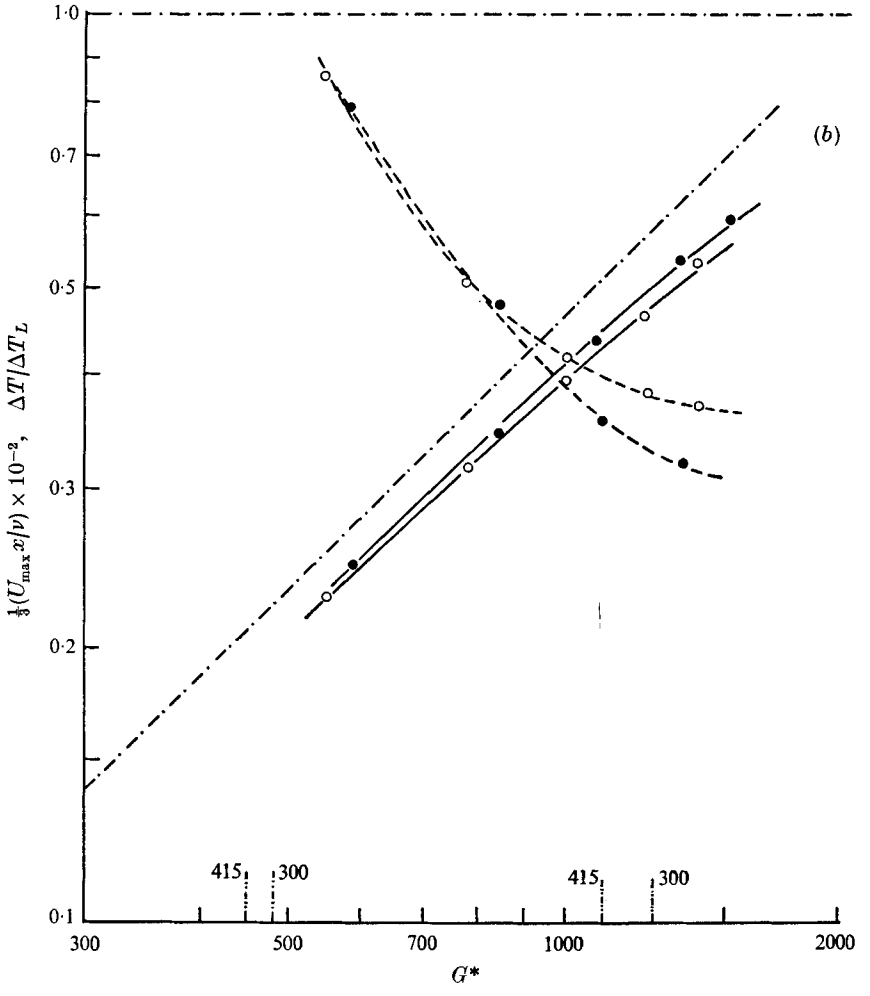


FIGURE 15. The variation of (*a*) the disturbance level and (*b*) the plate temperature excess and maximum mean velocity with $G^*$. –·–, calculated curves for laminar flow. Present data: ——, velocity; – – – –, temperature; –·–, boundaries of transition; ○, $q'' = 300$ B.Th.U./h ft$^2$; ●, $q'' = 415$.

and also by the success of stability analysis for this flow. Both the amplification of small disturbances and the frequency filtering by the boundary-region flow are calculated in terms of $G^*$ and much experimental evidence shows that these predictions are very accurate. However, as nonlinear effects begin to dominate, our results unequivocally indicate the failure of $G^*$.

Godaux & Gebhart (1974) suggested $G^*/x^{\frac{3}{5}}$ as the correlation parameter for the onset of what was defined as 'thermal' transition. This quantity has direct physical significance, being proportional to $[Q(x)]^{\frac{1}{5}}$, where $Q(x) = q''x$ is the total rate of thermal energy convection by the boundary region at $x$. They did not determine a corresponding parameter to characterize the end of transition. Our more detailed results indicate $G^*/x^n$, with values of $n$ of 0·4 and 0·54, respectively.

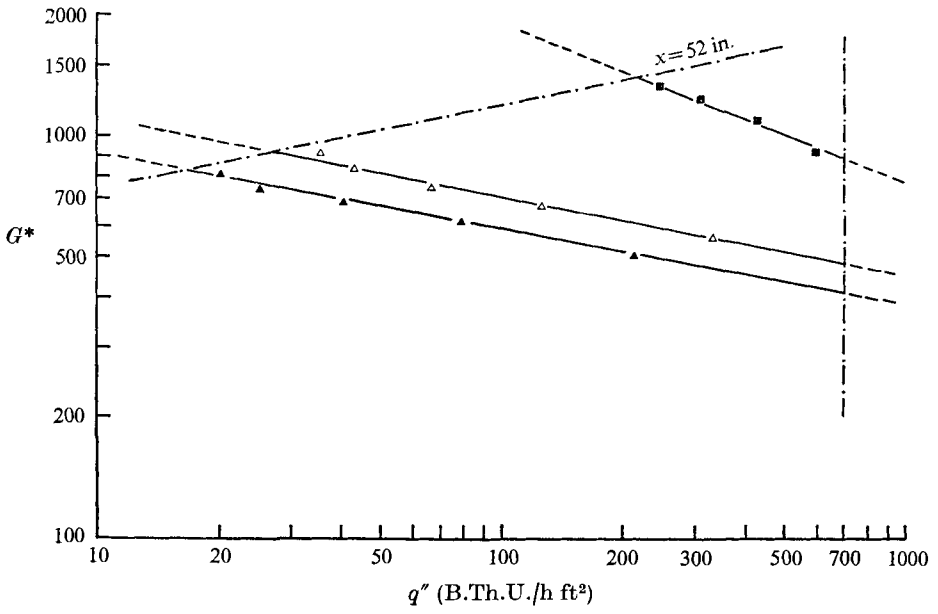


FIGURE 16. Boundaries of the transition regime. –·–, $x$ and $q''$ limits of the experiment; ▲, beginning of velocity transition; △, beginning of turbulent thermal mixing; ■, end of transition.

Other physical quantities, similar to $Q(x)$, might be significant in the transition process, for example, the local momentum flux $M$ in the boundary region, the kinetic energy flux $e$, the temperature difference across the boundary region $\Delta T$ and the characteristic velocity $U^*$. Each of these varies downstream as $G^*/x^n$, where $n$ is initially estimated as the value which applies for laminar flow. One may show that, for $M^{\frac{1}{3}}$, $n = \frac{1}{3}$, for $e^{\frac{1}{5}}$, $n = \frac{2}{5}$, for $\Delta t^{\frac{1}{4}}$, $n = \frac{3}{4}$ and for $U^{*\frac{1}{2}}$, $n = \frac{1}{2}$.

Since the mean temperature and velocity profiles deviate appreciably from the laminar ones only downstream of the beginning of transition, these values of $n$ are the correct estimates for $M$, $e$, $U^*$ and $\Delta T$ there and it is not unreasonable to expect that a parameter of the form $G^*/x^n$ may indicate the beginning of transition. The value of $n$ might conceivably lie somewhere between zero, as suggested by linear stability analysis, and the values indicated by these relations. A value of 0·4 for $n$ is not *a priori* unreasonable.

The above laminar relations for $M$, $e$, etc. are not valid late in transition. However, $[Q(x)]^{\frac{1}{5}}$ is still proportional to $(q''x)^{\frac{1}{5}}$, which results in $n = 0{\cdot}6$. Therefore, $Q(x)$ might be expected to dominate in the later stages of transition and in turbulent flow. Our value of $n$ is 0·54 for the end of transition, indicating a change from $n = 0{\cdot}4$ at the beginning of transition and perhaps leading to $n = 0{\cdot}6$ in complete turbulence. Apparently the dependence of $G^*$ on the surface heat flux is too weak.

Considering again the beginning of transition, for which our data indicate $n = \frac{2}{5}$, we find that the only prominent physical quantity, or combination of such quantities, which has this local variation at constant $q''$ is the fifth root of

the boundary-layer kinetic energy flux $e$. The form is $(e/\rho\nu^3)^{\frac{1}{5}} = F(Pr)\,G^*/x^{\frac{2}{5}}$, where $F(Pr)$ is a non-dimensional function known from the laminar similarity solution. A plausible interpretation of this consequence is that the kinetic energy flux of the mean flow is the energy available for disturbance growth and this, in turn, determines the onset of transition.

If $e/\rho\nu^3$ is non-dimensionalized in terms of $g$ and $\nu$ we obtain

$$e_0^{\frac{1}{5}} = \left[\left(\frac{\nu^2}{g}\right)^{\frac{2}{3}} \frac{e}{\rho\nu^3}\right]^{\frac{1}{5}} = \left(\frac{\nu^2}{gx^3}\right)^{\frac{2}{15}} F(Pr)\,G^*.$$

Rewriting this in terms of parameters $H$ and $E$ we have

$$e_0^{\frac{1}{5}}/F(Pr) = G^*(\nu^2/g\alpha^3)^{\frac{2}{15}} = G^*H^{\frac{2}{15}} = E.$$

From our measurements, $E = 13{\cdot}6$ and $15{\cdot}2$ for the beginning of velocity and thermal transition, respectively.

In order to assess any general validity of the parameter $E$, as a correlator of the beginning of transition, we have collected all transition data from the literature for flow adjacent to a vertical plate. The studies were performed in air, nitrogen, water and silicone oil and both the conditions of uniform flux and surface temperature occur. In each case we have calculated, as accurately as the reported data permit, the value of $E$ at estimated transition. The results are summarized in table 1. Data from the isothermal condition were reduced using $G$ instead of $G^*$ in $E$; see appendix. We see the surprising result that there is only about a 70 % spread in $E$ over a Prandtl number range from 0·7 to 11·85, including data for two different boundary conditions and several fluids.

Important variables in much of the data in the literature are the basis of judgement in the matter of assigning the location of transition and how the location was determined from the experiment. We ignored the data with $T_0 - T_\infty$ greater than about 50 °F owing to the uncertainty in property evaluation. Most studies define transition in terms of changes in quite gross features of the transport; for example, the mean velocity and temperature profiles. Our results indicate that such changes appear downstream of the first appearance of bursts. This undoubtedly explains many of the high values of $E$ in the table.

The parameter $E$ appears to be quite promising. So far it has also, at least approximately, absorbed the Prandtl number dependence which might arise owing to a varying relation of thermal and velocity boundary-region thicknesses. We should clearly like to investigate further the relevance and precision of $E$ through experiments designed to detect accurately first turbulence. Preliminary measurements in a new experimental study in our laboratory (Jaluria & Gebhart 1974), with a much shorter surface and in a different tank of water resulted in a value of $E$ of 13·1 for velocity transition, lending further support to the above analysis.

## 5. Conclusions

Our measurements during natural transition have determined the detailed behaviour of both the velocity and temperature fields. The mean profiles are in

| Reference | Basis of transition location | Fluid | Prandtl number | Boundary condition at surface | $E = G^*H^{\frac{2}{15}}$ | $E/E_p$† |
|---|---|---|---|---|---|---|
| Colak-Antic (1964) | Velocity | Air | 0·7 | Uniform heat flux | 15·7 | 1·16 |
| Polymeropoulos (1966) | Temperature | Nitrogen at high pressure | 0·72 | Uniform heat flux | 21·1 | 1·39 |
| Eckert & Soehngen (1951) | Temperature | Air | 0·72 | Uniform temerature | 20·7 | 1·36 |
| Warner (1966) | Temperature | Air | 0·7 | Uniform temperature | 22·2 | 1·46 |
| Cheesewright (1968) | Temperature | Air | 0·7 | Uniform temperature | 23·2 | 1·52 |
| Coutanceau (1969) | Temperature | Air | 0·7 | Uniform temperature | 20·0 | 1·32 |
| Knowles (1967) | Velocity | Silicone oil | 7·7 | Uniform heat flux | 16·2 | 1·19 |
| Lock & de B. Trotter (1968) | Temperature | Water | 9·8–11·85 | Uniform heat flux | 12·9–13·9 | 0·85–0·92 |
| Vliet & Liu (1968) | Temperature | Water | 3·6–10·5 | Uniform heat flux | 16·3–24·0 | 1·07–1·58 |
| Godaux & Gebhart (1974) | Temperature | Water | 6·4 | Uniform heat flux | 15·1–18·5 | 0·99–1·22 |
| Szewcyzk (1962) | Velocity | Water | 6·7 | Uniform temperature | 12·6 | 0·93 |
| Present study | Velocity | Water | 6·7 | Uniform heat flux | 13·6 | 1·0 |
| | Temperature | Water | 6·7 | Uniform heat flux | 15·2 | 1·0 |
| Other tank data (1973) | Velocity | Water | 6·7 | Uniform heat flux | 13·1 | 0·96 |

† $E_p$ in present study is either 13·6 or 15·2.

TABLE 1

good general agreement with the few past experimental studies of such flows. The measurements of the disturbance frequency, amplitude, growth rate and of the growth of turbulence in the boundary region clarify the sequence of events as the flow undergoes transition to complete turbulence.

Turbulence first appears in the velocity field. Resultant turbulent mixing of the more concentrated thermal region occurs further downstream and is apparent in increasing thermal turbulence. The initial turbulence is locally concentrated close to the peak of the laminar velocity profile. Downstream it diffuses outwards. The boundary region thickens and the mean profiles deviate progressively from the corresponding laminar ones. Transition events are expressed in terms of the two turbulence intermittency factors.

An important point that emerges from our results is that the Grashof number, or $G^*$, does not characterize the events of transition. We found that the parameter $G^*/x^n$, where $n$ is 0·4 and 0·54, correlates the two boundaries of the transition regime.

Another very significant observation concerns the nature of the interaction of the velocity and temperature fields during transition. The turbulence in the temperature field lags behind that in the velocity field, clearly a Prandtl number effect. The thickness of the temperature field never equals that of the velocity field. Predominant disturbance frequencies also lag behind. However, our two criteria for the end of transition, in terms of separate velocity and temperature intermittency factors and corresponding boundary-layer thicknesses, coincide, indicating that transition ends simultaneously in the two fields.

These results also agree with earlier studies of both the linear and nonlinear features of laminar instability. The disturbance frequency in the laminar portion of a flow undergoing transition was found to be still remarkably close to the filtered one predicted by linear stability analysis. The laminar disturbance growth rate was also found to agree with the earlier measurements of Jaluria & Gebhart (1973). In that controlled experiment an alternate spanwise steepening and flattening of the longitudinal mean velocity profile was found, as predicted to result from nonlinear three-dimensional disturbance interaction. A steepened profile might cause more rapid local disturbance growth and subsequent bursts in the region between the peak and the inflexion point of the laminar profile. A flattened profile, on the other hand, would carry momentum out across the outer portion of the boundary region and into the ambient fluid and, perhaps, thereby further destabilize the flow. However, our results indicate that bursts first appear close to the peak of the laminar velocity profile and we tentatively suggest that the steepened profile triggers transition.

The next step in the study of such flows would be an extensive local investigation of both the detailed events underlying the progress of the flow to developed turbulence and the early stages of complete turbulence. It would also be very important to measure turbulence parameters, both during transition and in complete turbulence. Our approximate correlation of transition in terms of $E$ also suggests a line of very practical further study.

The authors wish to acknowledge support for this research under National Science Foundation Grant GK 18529.

## Appendix

The most commonly employed definition of the Grashof number in natural convection flow is $Gr_x = g\beta_T x^3 \Delta T/\nu^2$, where $x$ is the downstream location, $\beta_T$ the coefficient of thermal expansion, $\nu$ the kinematic viscosity, $g$ the gravitational acceleration and $\Delta T$ the local temperature difference between the surface and the ambient fluid. Another parameter often used in such flows, $G$, is defined as $G = 4(\frac{1}{4}Gr_x)^{\frac{1}{4}}$. Both $Gr_x$ and $G$ can be used for arbitrary variation of $\Delta T$ with $x$.

For an isothermal surface in an unstratified medium, $\Delta T$ = constant. Similarly, it can be shown that, for a surface which dissipates a uniform heat flux $q''$, $\Delta T = Nx^{\frac{1}{5}}$. Further $N = (q''/k[-\phi'(0)])^{\frac{1}{5}}(4\nu^2/g\beta_T)^{\frac{1}{5}}$, where $k$ is the thermal conductivity of the fluid and $-\phi'(0)$ is a constant dependent on the Prandtl number. However, for a uniform-heat-flux surface another Grashof number is often defined as $Gr_x^* = g\beta_T x^4 q''/k\nu^2$, where $\Delta T$ has been replaced by $q''x/k$. The corresponding Grashof number parameter $G^*$ is defined as $G^* = 5(\frac{1}{5}Gr_x^*)^{\frac{1}{5}}$.

We have reported all our results in terms of $G^*$. In order to facilitate interpretation of our results in terms of other studies with an isothermal plate or with some other surface temperature variation, the following relation between $G$ and $G^*$ is derived: $G = G^*\{(0{\cdot}8)^4/[-\phi'(0)]\}^{\frac{1}{5}}$. For $Pr = 6{\cdot}7$, $[-\phi'(0)] = 1{\cdot}173$.

## REFERENCES


AUDUNSON, T. & GEBHART, B. 1975 Observations on the secondary mean motion induced by oscillations in a natural convection flow. To appear.

CHEESEWRIGHT, R. 1968 Turbulent natural convection from a vertical plane surface. *J. Heat Transfer*, **90**, 1.

COLAK-ANTIC, P. 1964 Hitzdraht messungen des Laminar-Turbulenten Umschlags bei freier Konvektion. In *Jahrbuch der WGLR*, p. 172.

COUTANCEAU, J. 1969 Convection naturelle turbulente sur une plaque verticale isotherme. *Int. J. Heat Mass Transfer*, **12**, 735.

DRING, R. P. & GEBHART, B. 1968 A theoretical investigation of disturbance amplification in external natural convection. *J. Fluid Mech.* **34**, 551.

DRING, R. P. & GEBHART, B. 1969 Hot wire anemometer calibration for measurement at very low velocity. *J. Heat Transfer*, **91**, 241.

ECKERT, E. R. G. & SOEHNGEN, E. 1951 Interferometric studies on the stability and transition to turbulence of a free convection boundary layer. *Proc. Gen. Disc. Heat Transfer, London.*

GEBHART, B. 1969 Natural convection flow, instability and transition. *J. Heat Transfer*, **91**, 293.

GEBHART, B. 1973 Instability, transition and turbulence in buoyancy induced flows. *Ann. Rev. Fluid Mech.* **5**, 213.

GODAUX, F. & GEBHART, B. 1974 An experimental study of the transition of natural convection flow adjacent to a vertical surface. *Int. J. Heat Mass Transfer*, **17**, 93.

GRIFFITHS, E. & DAVIS, A. H. 1922 The transmission of heat by radiation and convection. *Brit. Food Investigation Board, DSIR, London, Spec. Rep.* no. 9.

HIEBER, C. A. & GEBHART, B. 1971 Stability of vertical natural convection boundary layers: some numerical solutions. *J. Fluid Mech.* **48**, 625.

HOLLASCH, K. 1970 A survey of the literature, design and experimental verification of a measurement scheme for external turbulent natural convection flow. M.S. thesis, Cornell University.

HOLLASCH, K. & GEBHART, B. 1972 Calibration of constant temperature hot wire anemometers at low velocities in water with variable fluid temperature. *J. Heat Transfer*, **94**, 17.

JALURIA, Y. 1972 The growth and propagation of three-dimensional disturbances in laminar natural convection flow adjacent to a flat vertical surface. M.S. thesis, Cornell University.

JALURIA, Y. & GEBHART, B. 1973 An experimental study of nonlinear disturbance behaviour in natural convection. *J. Fluid Mech.* **61**, 337.

JALURIA, Y. & GEBHART, B. 1974 Stability and transition of buoyancy-induced flows in a stratified medium. *J. Fluid Mech.* **66**, to appear.

KLEBANOFF, P. S., TIDSTROM, K. D. & SARGENT, L. M. 1962 The three-dimensional nature of boundary-layer instability. *J. Fluid Mech.* **12**, 1.

KNOWLES, C. P. 1967 A theoretical and experimental study of the stability of the laminar natural convection boundary layer over a uniform flux plate. Ph.D. thesis, Cornell University. (See also KNOWLES, C. P. & GEBHART, B. 1969 An experimental investigation of the stability of laminar natural convection boundary layers. *Prog. in Heat Mass Transfer*, **2**, 99.)

LOCK, G. S. H. & TROTTER, F. J. DE B. 1968 Observations on the structure of a turbulent free convection boundary layer. *Int. J. Heat Mass Transfer*, **11**, 1225.

POLYMEROPOULOS, C. E. 1966 A study of the stability of free convection flow over a uniform flux plate in nitrogen. Ph.D. thesis, Cornell University. (See also POLYMEROPOULOS, C. E. & GEBHART, B. 1967 Incipient instability in free convection laminar boundary layers. *J. Fluid Mech.* **30**, 225.)

SZEWCZYK A. A. 1962 Stability and transition of the free convection boundary layer along a flat plate. *Int. J. Heat Mass Transfer*, **5**, 903.

TANI, I. 1969 Boundary layer transition. *Ann. Rev. Fluid Mech.* **1**, 169.

VLIET, G. C. & LIU, C. K. 1969 An experimental study of turbulent natural convection boundary layers. *J. Heat Transfer*, **91**, 517.

WARNER, C. Y. 1966 Turbulent natural convection in air along a vertical flat plate. Ph.D. thesis, The University of Michigan. (See also WARNER, C. Y. & ARPACI, V. S. 1968 An experimental investigation of turbulent natural convection in air at low pressure along a vertical heated plate. *Int. J. Heat Mass Transfer*, **11**, 397.)